THE JOURNAL OF PHYSICAL CHEMISTRY C

Article

Cite This: J. Phys. Chem. C 2020, 124, 2178−2192

pubs.acs.org/JPCC

Soft Nanocontainers Based on Hydroxyethylated Geminis: Role of Spacer in Self-Assembling, Solubilization, and Complexation with Oligonucleotide

Dinar R. Gabdrakhmanov,[†] Elmira A. Vasilieva,[†] Mikhail A. Voronin,[†] Darya A. Kuznetsova,[†] Farida G. Valeeva,[†] Alla B. Mirgorodskaya,[†] Svetlana S. Lukashenko,[†] Valery M. Zakharov,[‡] Alexander R. Mukhitov,[§] Dzhigangir A. Faizullin,[§,∥] Vadim V. Salnikov,[§,∥] Victor V. Syakaev,[†] Shamil K. Latypov,[†] Yuriy F. Zuev,[§,∥] and Lucia Ya. Zakharova*[,†]

[†]A.E. Arbuzov Institute of Organic and Physical Chemistry, FRC Kazan Scientific Center of RAS, Arbuzov street 8, Kazan 420088, Russia

[‡]Kazan National Research Technological University, 68, ul. K. Marx, Kazan 420015, Russia

[§]Kazan Institute of Biochemistry and Biophysics, FRC Kazan Scientific Center of RAS, Lobachevsky street 2/31, Kazan 420111, Russia

[∥]Kazan (Volga Region) Federal University, Kremlevskaya street 18, Kazan 420008, Russia

Supporting Information

ABSTRACT: Self-organization of hydroxyethylated gemini surfactants with different spacer fragments 16-s-16(OH) (s = 4, 6, 10, and 12) was studied in single solutions and in binary surfactant-oligonucleotide systems. Despite the fact that aggregation activity and solubilization capacity of aggregates decrease with an increase in spacer length, gemini with the longer spacer demonstrate superior binding capacity toward oligonucleotide as compared to single head surfactant and gemini analogs with shorter spacers. The detailed study testified that gemini with longer spacers are characterized by a looser packing mode, a moist and more polar interior, and tend to show polymorphism. These features in combination with favorable geometry factor providing suitable orientation of components are probably responsible for the beneficial lipoplex formation in the case of longer spacers. The effectiveness of oligonucleotide-surfactant complexation changes in the same order as transfection efficacy mediated by these gemini reported earlier [Zakharova, L. et al. Colloids Surf. B, 2016, 140, 269−277], which indicates that physicochemical aspects probably play a key role upon the design of nonviral vectors and may be used for prediction of transfection efficacy mediated by amphiphilic agents.

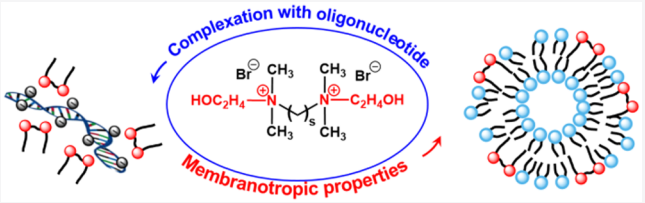

1. INTRODUCTION

Self-assembling systems based on surfactants can be considered as intermediates between organic and biological systems, since the latter are composed of building blocks resembling typical organic species, which are organized in much more complicated mode with secondary, ternary, and quaternary superstructures formed. Therefore, the study of self-assembling systems based on synthetic surfactants is a promising way to elucidate the molecular behavior of natural species. Another important issue responsible for the wide attention toward the surfactant systems is their application in bottom-up strategies,[1−5] mimicking principles of living systems, especially engineering of nanocontainers for drug and gene delivery. Formulations based on lipids and synthetic amphiphilic molecules are the most advanced alternative to natural carriers based on viruses. Simplicity of protocols and possibility for their large-scale production provide principle benefits for nonviral vectors over natural agents. In this field numerous studies, including our work, focus on cationic surfactants exhibiting high affinity toward negatively charged phosphate backbone of DNA.[6−16] Transfection efficacy has been summarized to increase markedly with the transition from conventional single head surfactants to gemini analogs; therefore, much attention has recently been paid to DNA complexation with dimeric cationic surfactants.[5] Two main aspects were highlighted in the literature, i.e., (i) structural behavior of lipoplexes, including their charge, size, and morphology characteristics, the mechanism of interactions, etc.; and (ii) correlation between chemical structure of surfactants and transfection efficacy. Those publications focused primarily on classical *m-s-m* surfactants. Meanwhile, modification of the chemical structure of both single head and dimeric surfactants (head groups and a spacer) is one of the

Received: October 28, 2019
Revised: December 22, 2019
Published: January 8, 2020

DOI: 10.1021/acs.jpcc.9b10079
J. Phys. Chem. C 2020, 124, 2178−2192

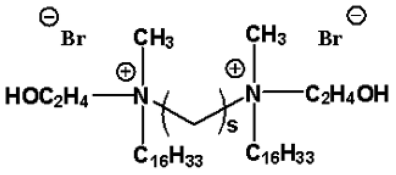

16-s-16(OH) (s=4, 6, 10, 12)

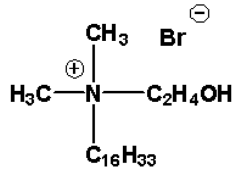

CHAB

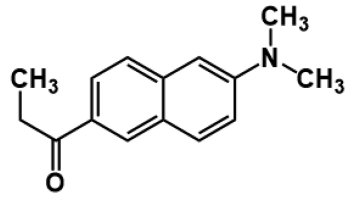

N,N-Dimethyl-6-propionyl-2-naphthylamine (Prodan)

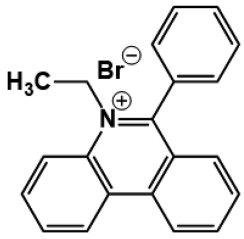

ethidium bromide (EB)

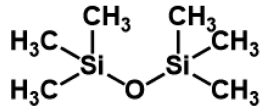

hexamethyldisiloxane (HMDSO)

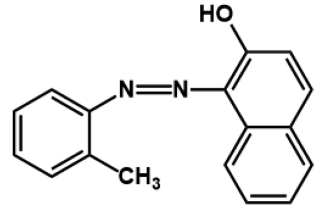

1-(*O*-tolyl-azo)-2-naphthol (Orange OT)

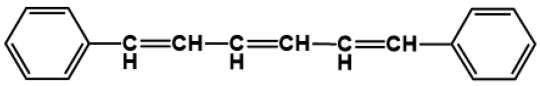

1,6-diphenyl-1,3,5-hexatriene (DPH)

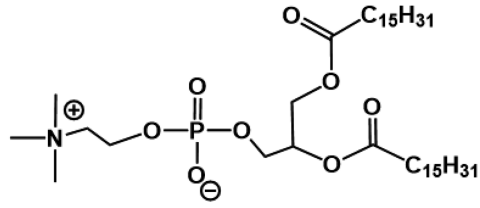

Dipalmitoylphosphatidylcholine (DPPC)

Figure 1. Chemical structures of compounds used.

ways to tailor their functionality, including binding capacity toward nucleotide moiety.[10−21]

The influence of headgroup structure on the complexation with DNA received much attention in literature including our work.[10−22] Along with ammonium gemini, their single head and dimeric analogs with imidazolium (Im), phosphonium (Ph), morpholinium (Mph), and diazabicyclooctane (DABCO) head groups were studied. The neutralization effect correlating with the contribution of electrostatic interactions of components enhances as follows for hexadecyl derivatives: Mph-16 ≈ DABCO-16 > Ph-16 ≈ CTAB > Im-16, with the latter demonstrating no recharging activity toward ONu.[10−12,16] Nontypical complexation was demonstrated for monocationic imidazolium surfactant and DNA decamer.[20] While strong binding of the components was revealed by the ethidium bromide exclusion assay, regardless of the alkyl tail length, no charge compensation occurred in the zeta potential measurement study, even at a high excess of surfactants. For imidazolium gemini surfactants, compaction and condensation effects toward DNA were testified, contributed by multicentered interactions of components including $\pi-\pi$, electrostatic, and hydrogen bonding, which was accompanied by conformational changes in the system.[17] For a series of imidazolium gemini with polymethylene and thioether spacers, strong complexation with DNA was established within low surfactant concentrations due to the premicellar self-assembly.[18,19] This is probably responsible for low cytotoxicity of lipoplexes demonstrated by the MTT test. A series of dimeric and oligomeric surfactants with pyridinium head groups was designed as effective DNA carriers. The variation of hydrophobicity, the nature of spacer and counterions was documented to be the effective way for optimization of structure−activity correlation and balance between transfection efficacy and toxicity.

From the viewpoint of the role of headgroup, the introduction of fragments capable of hydrogen bonding into amphiphilic matrix[22−31] should specially be emphasized. The lipoplex formation due to synergistic contribution of electrostatic forces and hydrogen bonding is documented for gemini with ammonium head groups bearing an ester fragment in the spacer, with the compaction effect increasing with an increase in surfactant tail length.[22] Structural behavior of gemini can be varied by the introduction of hydroxy-groups into the spacer. This resulted in closer packing of the surfactant in aggregates, which correlated with the number of hydroxy-substituents.[28] Hydroxyalkylated surfactants are reported to demonstrate benefits in both aggregation and functional activity.[23,24] In ref 23, the homological series of hydroxyalkylated ammonium surfactants was studied, with a decrease in critical micelle concentration (cmc) observed with the introduction of the

DOI: 10.1021/acs.jpcc.9b10079
J. Phys. Chem. C 2020, 124, 2178−2192

hydroxyalkyl moiety compared to unsubstituted analogs. Functional activity of these surfactants, e.g., catalytic effect of micellar and microemulsion systems toward the ester hydrolysis, is contributed by both electrostatic interactions and hydrogen bonding surfactant/reagents and varied as follows: trimethylammonium < hydroxypropylated < hydroxyethylated headgroup.[23,24] Similarly, DNA interaction with trimethylammonium surfactants can be essentially modulated through successive replacement of methyl groups by the hydroxyethyl moiety.[27] The results were treated in terms of changes in surfactant packing mode and surface curvature influencing the access of head groups to the complexation with DNA. Importantly, that less cytotoxicity was revealed for the more polar surfactants. The role of nonelectrostatic interactions in the lipoplex formation is emphasized,[31] with little if any effect of the polarity of head groups observed on the compaction of DNA macroions. These findings are in line with the beneficial efficacy of pegylated formulations in the drug and gene delivery, since hydroxyethyl fragments are the monomeric units of biocompatible polyethylene glycols widely used for the surface modification and protection of nanocarriers. Meanwhile gemini-bearing hydroxyethyl fragments are scarcely explored compared to single-head analogs.

Upon the analysis of the structure−activity relation, much attention was paid to the role of the spacer.[32−39] Superior results were obtained for ethanediyl- and propanediyl versus the longer $(-CH_2)_5$ and $(-CH_2)_{12}$ polymethylene spacers,[37] while the gemini with the pentadiyl spacer appeared the most effective in the work.[36] Complicated dependence of DNA transfection on the spacer length was obtained,[34] where an increase in gene transfection occurred with the transition from propanediyl to pentanediyl, while further increase in spacer length resulted in worse activity. In turn, pseudoglyceryl gemini with oxyethylene spacer displayed advanced transfection efficacy over the analogs with the polymethylene spacer.[35] It should be emphasized that the role of spacer may be indirectly realized through the influence on aggregation behavior of surfactants. Therefore, this aspect should be taken into account as well. Spacer nature is reported to markedly affect the size and morphological behavior of gemini.[40−43] To answer the criteria of low toxicity and biocompatibility, much attention is paid to gemini with natural fragments, such as arginine- and amino acid-based dimeric surfactants, with essential influence of spacer length on the structural behavior of aggregates demonstrated.[44,45]

Importantly, despite the abundant data summarized above, high interest in the design of novel surfactants and evaluation of them as gene carriers have been currently preserved and enhanced.[13−15,46−54] Intensive efforts have focused on the structure−activity relations between the gene transfection properties and chemical structure of carriers. A variety of novel gemini surfactants were designed and tested as nonviral vectors. While excellent results were achieved in compaction and charge neutralization of DNA molecules in the presence of single gemini, their transfection efficacy was moderate. To improve it, amphiphilic carriers based on metallosurfactants, polycationic matrix, and functionalized with natural fragments are designed. Another promising way is the use of helper lipid molecules or the PEGylation of lipoplexes.

The above brief review shows that the following factors should be considered upon analyzing the DNA transfection mediated by surfactants: (i) the binding capacity of amphiphiles toward DNA; (ii) the compaction of polyanions of nucleic acids (the size of lipoplexes); (iii) the charge neutralization of DNA; (iv) the penetration of lipoplexes through cell membranes; and (v) the viability of cells treated. Most of these events are controlled by the structural behavior of surfactants, in particular, their aggregation activity, morphology, surface potential, solubilization capacity, etc. The present work is a continuation of our studies focusing on the complexation of cationic surfactants with oligonucleotide and DNA.[10−16,29,30,55−57] The promising results were obtained for DNA transfection by gemini bearing hydroxyethylated head groups 16-s-16(OH) (Figure 1), with the spacer length playing key role.[29,30] These gemini demonstrated advanced properties as compared to their 16-s-16 unsubstituted counterparts and single-head analogs. Meanwhile, the latter are well-studied and their functional activity documented, whereas few works are available on the structural behavior of hydroxyalkylated gemini,[25,26] with extremely scarce information reported on their functional activity. To shed light on the structural behavior of these gemini and the origin of high transfection efficacy of lipoplexes reported in ref 29, the present work is devoted to their solution behavior, and solubilization activity, as well as interaction with the DNA decamer. Special attention is paid to the gemini with longer spacers showing the highest efficacy to elucidate the source of beneficial behavior of these amphiphiles.

2. MATERIAL AND METHODS

2.1. Materials. All reagents used were of analytical grade. Solvents were dried if necessary by standard methods. 1-(*O*-Tolyl-azo)-2-naphthol (Orange OT) (Sigma-Aldrich), ethidium bromide (EB) (Sigma-Aldrich), hexamethyldisiloxane (HMDSO) (Sigma-Aldrich), adenosine triphosphate (ATP) (Sigma-Aldrich), cetylpyridinium bromide (CPB) (AppliChem, BioChemica, Germany) and pyrene for fluorescence (Sigma) (≥99%) were used as received. Double-stranded palindromic DNA decamer $d(GCGTTAACGC)_2$ (molecular weight is 3028 g/mol) was purchased from Joint Stock Company Syntol (Moscow, Russia).

2.2. Synthesis. Cetyl hydroxyethyl dimethylammonium bromide (CHAB) and gemini were synthesized through reaction of cetyl bromide with 2-dimethylaminoethanol or by quaternization of hydroxyethylmethylcetylamine by polymethylene dibromide, in analogy with refs 58−60. The structure and properties are confirmed by NMR, IR spectroscopy, and elemental analysis (see refs 29 and 30).

2.3. NMR Experiments.[61−64] All NMR experiments were performed on a Bruker AVANCE-600 spectrometer operating at 600.13 for the ^1H. The spectrometer was equipped with a Bruker multinuclear z-gradient inverse probe-head capable of producing gradients with strength of 50 G cm^{-1}. All experiments were carried out at 30 ± 0.2 °C. Chemical shifts (CSs) were reported relative to HDO (4.7 ppm) for ^1H. Experimental details are given in the Supporting Information. The molecular structures for calculation of hydrodynamic radii were generated using molecular modeling program CS Chem3D Ultra 6.0 (CambridgeSoft Corp, http://www.camsoft.com).

The pulse programs for all NMR experiments were taken from the Bruker software library.

2.4. Dynamic Light Scattering Measurements. Dynamic light scattering (DLS) measurements were performed by means of Malvern Instrument Zetasizer Nano. The measured autocorrelation functions were analyzed by the

DOI: 10.1021/acs.jpcc.9b10079
J. Phys. Chem. C 2020, 124, 2178−2192

Malvern DTS software and second-order cumulant expansion methods. The effective hydrodynamic radius (R_H) was calculated according to the Stokes−Einstein equation: $D_S = k_B T/6\pi\eta R_H$, in which D_S is the diffusion coefficient, k_B is the Boltzmann constant, T is the absolute temperature, and η is the viscosity. Zeta potential Nano-ZS (MALVERN) using laser Doppler velocimetry and phase analysis light scattering was used for zeta potential measurements. The temperature of the scattering cell was controlled at 25 °C; the data were analyzed with the software supplied for the instrument. DLS and zeta potential titration involved no less than seven measurements in ten runs. Only multiply reproducible results were taken into account, thereby they differed by less than 3%.

2.5. FTIR Spectroscopy. Transmission infrared spectra of gemini surfactants solutions were recorded using IRAffinity-1 (Shimadzu) FTIR spectrophotometer equipped with a DLATGS detector. Surfactant solutions (5 mM in D_2O) were placed in a demountable CaF_2 transmission cell with a 100 μm path length. Solutions were thermostated at 25 ± 0.1 °C. For each spectrum, 256 scans in the spectral range of 4000−1000 cm^{-1} were averaged at a spectral resolution of 4 cm^{-1}. The solvent absorption and contributions from residual water vapor were compensated by computer subtraction techniques. Spectra were unsmoothed. For the sake of comparison, all the spectra were normalized on the absorption intensity of the methylene stretching vibrations band at 2920 cm^{-1}.

2.6. Solubilization of Orange OT. The solubilization experiments were performed by adding an excess of crystalline dye to solutions. These solutions were allowed to equilibrate for about 48 h at room temperature. They were filtered, and their absorbance was measured at 495 nm (molar extinction coefficient 17400 L mol^{-1} cm^{-1}) using Specord 250 Plus spectrophotometer. Quartz cuvettes containing the sample were used, with a cell length of 0.1−0.5 cm. The dye solubilization data may be used for the estimation of molecular masses and aggregation numbers of micelles[65] on the assumption that the probe is insoluble in aqueous surfactant solution below the cmc, while beyond cmc one dye molecule is bound by a micelle. The absorbance versus concentration plot can be analyzed in terms of linear equation $C = \text{cmc} + b \times D$, where C is surfactant concentration above cmc (g/L), b is the slope of dependence, and D is the absorbance of saturated solution of Orange OT at 495 nm. Molecular mass of micelle (MMm) is calculated as follows: $\text{MMm} = b \times l \times \varepsilon$, where l is the light path length and ε is the molar extinction. The aggregation numbers N_{agr} are determined by division of MMm by the molecular mass of a surfactant molecule.

2.7. Micropolarity Study with the Use of Fluorescent Dye Prodan. Samples with the concentration of 16-s-16(OH) 10 μM and concentration of Prodan 5 μM were prepared and fluorescence spectra were recorded at 370−650 nm and 25 °C in a Varian Cary Eclipse spectrofluorimeter. Sample excitation was at a wavelength of 335 nm.

2.8. Fluorescent Spectroscopy with the Use of Fluorescent Probe DPH. Steady-state fluorescence anisotropy of DPH was measured on a Cary Eclipse (USA) spectrometer equipped with filter polarizers. DPH were excited at 361 nm, and the fluorescence intensity was measured at 450 nm. The excitation and emission slit widths were 2.5 and 5 nm, respectively. Calculation of the parameter of anisotropy is based on the relationship $r = (I_v - I_h)/(I_v + 2I_h)$, where I_v and I_h are the intensity of fluorescence of the vertically and horizontally polarized emission in case of excitation of samples by the vertically polarized light. The embedded software automatically determined the correction factor and anisotropy value. A quartz cell of 1 cm path length was used for all fluorescence measurements. A temperature of 25 °C was maintained. Surfactant solutions were prepared by the stepwise dilution of a stock sample, with a wide concentration range from molecular solution to 50 mM covered. Fixed concentration of fluorescence probe DPH of 0.175 mM was used.

2.9. Fluorescence Spectroscopy with the Use of Fluorescent Probe Pyrene.[66−68] The fluorescence spectra of pyrene (1×10^{-6} mol L^{-1}) in surfactant solutions in the absence of and the presence of a quencher (cetylpyridinium bromide) were recorded at 25 °C in a Varian Cary Eclipse spectrofluorimeter. Sample excitation was at a wavelength of 335 nm. Emission spectra were recorded in 350−500 nm. The thickness of the cell was 10 × 10 mm. The scanning speed was 120 nm/min. Additional details are given in the Supporting Information.

2.10. Turbidity Measurements. The phase transition of surfactant/DPPC mixtures was studied using Lambda 25 (PerkinElmer) and Specord 250 Plus double-beam spectrophotometers, equipped with a Peltier thermostated cell holder, using quartz cells of 1 cm path length. Before turbidity measurements, the samples were diluted to 7×10^{-4} M DPPC concentration in Tris-HCl buffer (4×10^{-3} M; pH = 8.0). The reference cell was filled with a buffer solution. The sample cells were capped to prevent evaporation. Turbidity was measured at 350 nm and expressed in absorbance. Turbidity values were recorded as a function of temperature with the sample continuously stirred during heating. The heating rate was 0.1 °C/min, with the temperature varied between 35 and 45 °C. Small volumes of concentrated surfactant were added to the same sample, and temperature scans were repeated. Turbidity traces were approximated by the Van't Hoff equation for the two-state model yielding half-transition temperature values.

2.11. Ethidium Bromide (EB) Exclusion Study. Fluorescence spectra of ONu-EB complexes were recorded on a Varian Cary Eclipse spectrofluorimeter (Germany), within the range of 500 to 700 nm, at 25 °C. The excitation and emission wavelengths were 480 and 615 nm, respectively. Sample preparation is given in the Supporting Information.

2.12. Transmission Electronic Microscopy (TEM). The prepared suspensions (equimolar surfactant-ONu mixture in Tris/HCl buffer, 4 mM, pH = 8.0) were processed by using copper grids to adsorb aggregated particles from the suspension. The specimen was observed under a JEM 1200EX transmission electron microscope (JEOL, Japan) operated at 80 kV. Experimental details are described in ref 56.

2.13. Confocal Microscopy. For localization of the oligonucleotide we have used the Hoechst 33342 dye (0.1 mg/mL). This dye binds to double-stranded DNA with a preference for domains enriched with adenine and thymine. Confocal images were collected with laser confocal microscope LSM 510 META (Carl Zeiss) using a 63× oil immersion lens (1,4 NA). Preparations were viewed by using the UV Argon laser (Coherent Inc.) line (351 nm). The emitted light was detected through a band-pass filter (420−550 nm). For visualization of surfactant globules, we used a HeNe laser line (533 nm) and the transmitted light-imaging mode.

DOI: 10.1021/acs.jpcc.9b10079
J. Phys. Chem. C 2020, 124, 2178−2192

Table 1. Summary of the Tensiometry, Fluorimetry, and Dye Solubilization Data toward Orange OT: cmc Values, Surface Excess (Γ_{Max}), Surface Area Per Head Group (A_{min}), Solubilization Power (S), and Aggregation Number (N_{agr}) for 16-s-16(OH) Amphiphiles

	cmc, μM[a]						
s	tensiometry	fluorimetry	dye solubilization	Γ_{max}, mol m^{-2}	A_{min}, nm^2	10^3 S	N_{agr}[b]
4	1.4	0.83	5	2.19	0.76	29.0	12 (7)
6	9.5	0.75	8	2.10	0.79	36.5	18 (2)
12	8.0	1.30	13	1.84	0.90	16.0	28 (1.8)

[a]The cmc = 27 and 43 μM for unsubstituted analogues 16-4-16 and 16-6-16, respectively.[83] [b]Aggregation numbers obtained by dye solubilization technique and pyrene fluorescence quenching (in the brackets).

3. RESULTS AND DISCUSSION

3.1. Aggregation Behavior of Single Surfactant Solutions. Aggregation of gemini in aqueous solution is widely investigated including the *m-s-m* family.[40−45,69,70] The nature of spacer was documented to affect both the cmc value and morphology of aggregates.[70−76] The cmc values for *m-s-m* gemini were reported to have a maximum of s = 4−6, while aggregation numbers decreased with an increase in spacer length.[70,76] For the monomethylene spacer, small micelles composed of ca. 30 monomer units were documented, while larger aggregates with aggregation number of 50 occurred in the case of s = 4.[41] For the ethanediyl spacer, the sphere-to-rod transition was revealed,[70,77] which is probably due to the increase in counterion binding and dehydration of head groups.[78−80] Rigid spacer bearing unsaturated moiety can be responsible for the formation of small micelles with sizes of ca. 2 nm.[42] The comparison between the effects of spacer length and rigidity revealed that spacer length plays the prior role.[43]

By contrast to this, scarce information is available for the hydroxyethylated counterparts.[58−60,81] Therefore, different techniques were involved herein to elucidate aggregation behavior of the 16-s-16(OH) series. Figures S1−S3 show data obtained by tensiometry and fluorescence probe techniques, i.e., by two generally accepted methods. Tensiometric cmc values summarized in Table 1 are in good agreement with few available data for the 16-4-16(OH) surfactant (cmc of 1.8[25] and 2.5[26] μM). At the same time, some lower cmcs were obtained by fluorimetry (Table 1). Such a discrepancy can be due to the formation of premicellar aggregates that can be sensed by fluorescence technique. Pyrene and surfactant may also self-associate into small aggregates that do not exist in the absence of pyrene.[82] This result is in line with low aggregation numbers calculated according to eq (S3) of Figure S3; N = 7, 2, and 2 for a spacer denoted as s = 4, 6, and 12, respectively, at the concentrations that not very much exceed cmc. Although much higher N values are also reported,[25] this result does not contradict with literature data, since concentrations much higher than cmc were used therein. For example, N = 420 and 170 were obtained for 16-4-16(OH) and 16-6-16(OH) at a concentration of 50 mM.[25] Analysis of tensiometry data in terms of eqs S1 and S2 demonstrates that adsorption characteristics Γ_{max} and A_{min} depend on spacer length. Closer packing of molecules at the interface occurs in the case of shorter spacer with s = 4, 6.

3.2. NMR Self-Diffusion Study. To obtain detailed information on the association behavior of amphiphiles, the NMR self-diffusion technique was used. Experimental data were analyzed in the framework of the two-site model[84,85] based on the difference of intrinsic self-diffusion coefficients (D_S) for the surfactant monomers and micelles. The translational mobility of a surfactant essentially decreases (by 1−2 orders of magnitude), when it is diffused with the micelle.

Since there is a fast exchange in the NMR time scale between surfactants in the micelles and in the bulk phase, the following two-site bound-free model applies: $D_{obs} = D_{agr}P_{mic} + D_{mon}(1 - P_{mic})$, where D_{obs} represents the exchange-averaged diffusion coefficient, P_{mic} is the fraction of micellized surfactant molecules, D_{agr} is the diffusion coefficient of the micelle, and D_{mon} is the diffusion coefficient of the monomer surfactant in the aqueous phase.

Essential experimental data are summarized in Table 2 (all details are in Figures S4−S7). Due to the low aggregation

Table 2. NMR Self-Diffusion Data for Different 16-s-16(OH) (s = 4, 6, 12) Concentrations in Aqueous Solution: Self-Diffusion Coefficient (D_S), Effective Hydrodynamic Radius (R_H), and Aggregation Numbers (N_{agr})[a]

C, mM	$D_S \times 10^{-10}$ m^2/s	R_H, A	N_{agr}	D_S, HMDSO
16-4-16(OH)				
0.05	0.87	32.0	75	–
0.1	0.67	41.5	163	0.91
0.5	0.63	44.1	196	0.86
1.0	0.43	64.7	617	0.44
2.0	0.45	61.8	538	0.47
3.0	0.46	60.4	504	0.47
10	0.47	59.2	472	0.48
16-6-16(OH)				
0.01	1.1	25.3	33	–
0.05	0.93	29.9	55	0.90
0.1	0.81	34.3	84	–
0.5	0.66	42.1	154	1.23
1	0.64	43.4	169	0.95
2	0.63	44.1	177	0.81
3	0.62	44.8	186	0.68
5	0.63	44.1	177	0.62
10	0.59	47.1	216	0.62
16-12-16(OH)				
0.01	2.63	10.6	2	–
0.05	0.96	29.0	31	–
0.1	0.82	33.9	49	–
0.5	0.73	38.1	69	–
1	0.72	38.6	72	0.81
2	0.64	43.4	103	0.71
3	0.65	42.8	98	0.72
5	0.65	42.8	98	0.69
10	0.61	45.6	119	0.62

[a]N_{agr} are calculated from theoretical values of $R_{H,mon}$ = 7.6, 7.9, and 9.3 A for 16-4-16(OH), 16-6-16(OH), and 16-12-16(OH), respectively.

DOI: 10.1021/acs.jpcc.9b10079
J. Phys. Chem. C 2020, 124, 2178−2192

threshold of the surfactants and very low signal-to-noise, we failed to measure their cmc values and reliable D_S values of monomeric gemini. Therefore, theoretical self-diffusion coefficients, $D_{S,theor}$ based on the bead model approximation[86] were used for gemini with s = 4, 6, and 12, respectively.

These NMR data prove that surfactants are in the aggregated state within the concentration range used in the study, with their sizes markedly changing only at low concentration, while further tending to saturate on the level of ca. 45−50 Å. Some decrease in the plateau value of aggregate sizes is observed with an increase in the spacer length. It can be assumed that this is due to the closer packing of surfactant molecules with longer spacer capable of folding inside the micelles. This in turn is in line with formally lower aggregation numbers of 16-12-16(OH) aggregates, since the spacer fragment located in the micellar core prevents the incorporation of additional surfactants at the given aggregate size. In this case, the longer the spacer fragment, the closer packing occurs on the palisade layer of micelles, while the Stern layer and micellar interior could be looser and more disordered. Somewhat higher D_S values of the hydrophobic probe HDMSO are also in accordance with this assumption, supporting the lability of the probe within the micellar core. The use of the less hydrophobic probe, benzyl alcohol, does not markedly change aggregation characteristics of aggregates, even at the 5-fold increase in the guest concentration. From dependence of, e.g., the 16-4-16(OH) ^{1}H chemical shifts versus concentration of benzyl alcohol, one can conclude that the most notable changes take place for the headgroup protons of gemini (Figures S8). This is typical for all the gemini studied, thereby indicating the solubilization of the probe in the palisade zone of aggregates and simultaneously emphasizing the similarity of their local microenvironmental characteristics therein.

Calculated aggregation numbers (Table 2) may serve as an appropriate supplement to those obtained by fluorescence and dye solubilization techniques (Table 1). While low aggregation numbers are revealed near cmc by these techniques, much higher values are observed upon the increase in surfactant concentration (472, 216, and 119 at 10 mM for 16-4-16(OH), 16-6-16(OH), and 16-12-16(OH), respectively). These results are close to those obtained by other authors.[25]

3.3. Size and Zeta Potential Study. Dynamic light scattering and zeta potential data (Figure 2) exemplified by 16-12-16(OH) reveal populations at about 7 nm (concentration of 70 cmc) and ca. 20 nm (concentration of 400 cmc). This is in reasonable agreement with NMR self-diffusion data, which testify to the formation of aggregates with R_H up to 4 to 6 nm, with an increase in their sizes observed at higher concentration. Zeta potential measurements show that an increase in zeta potential occurs from +40 to +80 mV with an increase in surfactant concentration. This is in line with an increase in aggregation numbers (Table 2) and ref 25.

3.4. Fluorescence Spectroscopy Measurements. Application of fluorescent dyes may provide valuable information on microheterogeneous systems.[87−91] To specify the morphology of aggregates, fluorescence spectroscopy based on the measuring of anisotropy (r) of spectral probes, e.g., DPH can be used[89−91] to testify an internal structure of aggregates, in particular, the surfactant packing mode. Lower r values indicate the less-ordered state, while the higher r provides evidence for the closer packing of monomers. Generally, the r value close to 0.2 indicates that close packing occurs typical for vesicular

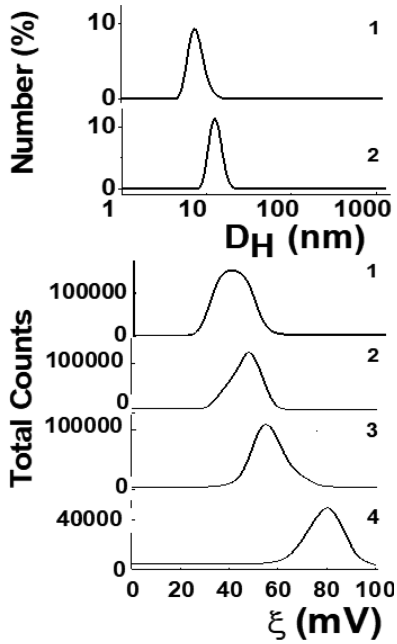

Figure 2. Number-averaged size distribution for the 16-12-16(OH) solution at different concentrations (1−0.075 mM, 2−0.4 mM); zeta potential data for 16-12-16(OH) solution at concentrations of 5 (1); 75 (2); 150 (3); and 400 (4) μM; 25 °C.

aggregates, while $r \leq 0.1$ indicates the micelle-like aggregate occurrence.[89−91] Figure 3 shows the anisotropy data

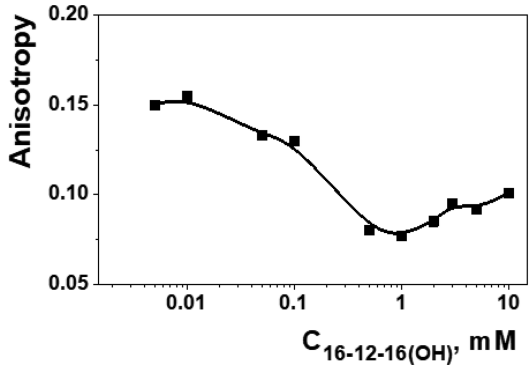

Figure 3. Variation of fluorescence anisotropy r of fluorescence probe DPH as a function of 16-12-16(OH) concentration; 25 °C.

exemplified by 16-12-16(OH) gemini. Within the lower concentration, r value is close to 0.15, which allows us to assume rather close packing of surfactants, e.g., layered ordering. Further increase in concentration is accompanied by a decrease in the anisotropy parameter to 0.08−1.0, indicating the formation of a micelle-like aggregate, which is in agreement with DLS and NMR data. This indicates that the gemini with the longest spacer tends to display polymorphism, which agrees with different values of the packing parameter reported earlier.[29]

3.5. Micropolarity Study with the Use of Fluorescent Dye Prodan. To compare the microenvironmental characteristics of the gemini surfactants, solvatochromic probes are usually used.[92−95] For this purpose, fluorescent dyes highly sensitive to micropolarity, such as Prodan, are widely used. This dye is characterized by a large dipole moment in the excited state due to charge transfer from amino to carbonyl

DOI: 10.1021/acs.jpcc.9b10079
J. Phys. Chem. C 2020, 124, 2178−2192

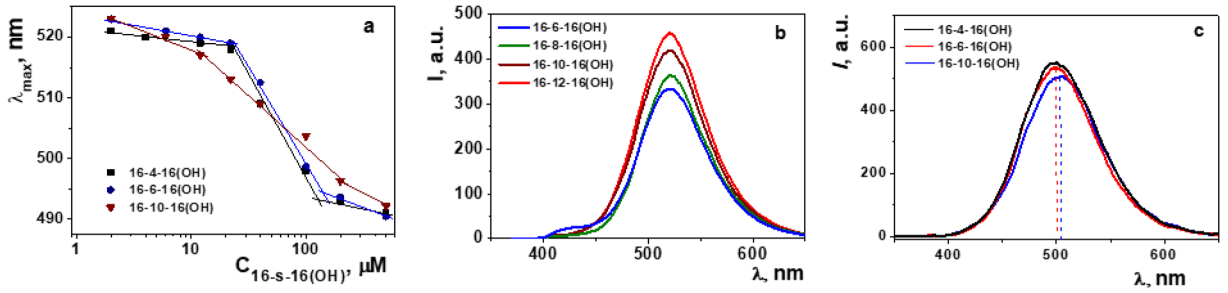

Figure 4. (a) Maximum of fluorescence intensity of Prodan versus surfactant concentration plot for 16-*s*-16(OH) (*s* = 4, 6, and 10); (b) emission fluorescence spectra of Prodan for 16-*s*-16(OH) (*s* = 6, 8, 10, and 12) within the concentration range before cmc; and (c) emission fluorescence spectra of Prodan for 16-*s*-16(OH) amphiphiles (*s* = 4, 6, and 10) within the concentration range above cmc.

groups, which is responsible for the effect of solvent polarity on the stabilization/destabilization of excited state. Unlike highly hydrophobic dyes, e.g. Nile red, Prodan is capable of partitioning between the phases with different polarity, thereby being sensitive to changes in location and structural rearrangement, which is of importance for microheterogeneous systems. Typically, empirical E_T parameter is used to characterize the polarity of media, which linearly correlates with the value of maximum of the emission spectra. Therefore, this dye was used to compare the micropolarity of aggregates formed in the 16-*s*-16(OH) systems.

Figure S9 and Figure 4 show emission spectra of Prodan and concentration dependences of the maximum of fluorescence intensity. In all cases, blue shift occurs indicating the change in microenvironmental characteristics of the probe due to its solubilization in less polar micellar interior. Critical concentrations on the plot (Figure 4a and Table S1) corresponding to a sharp change in the spectrum maximum are much higher compared to cmc obtained by alternative techniques (Table 1). This probably reflects the facts that (i) micellar aggregates formed just near the cmc show low solubilization capacity and (ii) Prodan partitions between the phases rather than being completely bound by aggregates.

Figure 4b shows emission spectra of gemini, which testify that no shift of spectrum maximum occurred with changes in spacer length within the concentration range before cmc. At the same time, above the cmc a blue shift is observed with an increase in surfactant concentration, which varies with the length of the spacer fragment (Figures 4c and S9). Spectral maximum shifts from 520 nm to 490, 498, and 508 nm for 16-4-16(OH), 16-6-16(OH), and 16-12-16(OH), respectively, at 100 μM. This indicates that micropolarity of the probe increases with an increase in spacer length. Meanwhile, an increase in intensity of fluorescence is observed with an increase in spacer length before cmc and the opposite trend occurs in micellar systems. Two reasons could be considered in this connection. The most trivial explanation is the change in solubility of Prodan in solution of gemini with different spacers. In the case of micellar systems (Figure 4c), this correlates well with the difference in micropolarity, i.e., the highest polarity revealed for 16-6-16(OH) provides the worst favorable affinity to nonpolar dye. In addition, it can be assumed that association of dye is responsible for the change in the fluorescence intensity. This idea was proved in work[93] on the example of absorption spectra of Prodan. At the same time, the authors specified that unlike absorption spectra, the emission spectra of Prodan show low sensitivity to the probe association.

3.6. Solubilization of Hydrophobic Probe Orange OT.

Additional information on the micellar properties may be obtained from the dye solubilization study. Orange OT is a water-insoluble dye, and the appearance of the absorbance at 495 nm (Figures 5 and S10) indicates that the solubilization of

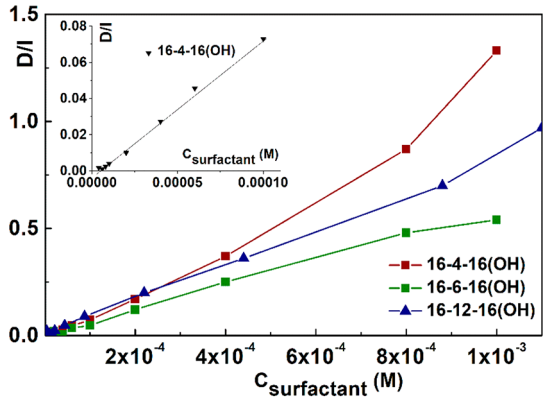

Figure 5. Absorbance of Orange OT reduced to a 1 cm cuvette (D/l) versus surfactant concentration; 25 °C; λ = 495 nm. Inset exemplifies the low concentration range for 16-4-16 (OH) gemini.

the probe in nonpolar interior of aggregates occurs. Table S2 summarizes C_{cr} values corresponding to the sharp increase in the absorbance at 495 nm (Figure 5). Typically, this breakpoint is considered as an onset of the aggregation. As can be seen from Table S2, the valuable increase in absorbance occurs at rather high surfactant concentrations, much exceeding the tensiometry cmcs. These critical points probably correspond to the formation of true micelles capable of retaining the dye molecules. At the same time, the analysis of the low concentration range (Figure 5, inset, and Figure S10) reveals cmc values close to those obtained by tensiometry (Table 1). This supports the assumption on different types of aggregates (premicellar aggregates and true micelles) formed in the surfactant solutions that can be sensed by different techniques. This is probably due to a very low aggregation threshold of gemini surfactants, so that fluorescence ratiometry reflects the association process beginning with premicellar aggregates, while other methods selectively sense the true aggregates. In fact, calculations of aggregation numbers based on solubilization data give the higher *N* values from 12 to 30 as compared to fluorescence measurements (Table 1). Besides, unlike with fluorimetry results, aggregation numbers obtained from solubilization data increase with an increase in spacer length.

DOI: 10.1021/acs.jpcc.9b10079
J. Phys. Chem. C 2020, 124, 2178−2192

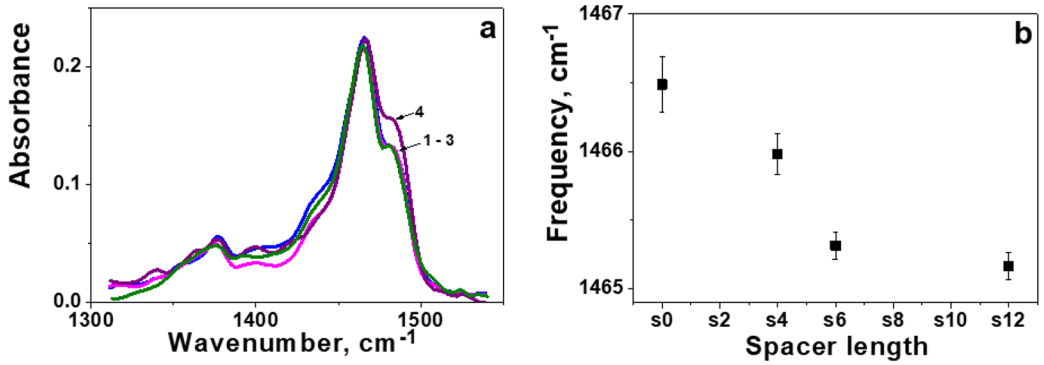

Figure 6. (a) FTIR spectra of hydroxyethylated gemini surfactants with increasing spacer length "*s*" in solution: (1) *s* = 4, (2) *s* = 6, (3) *s* = 12. *S* = 0 (4) conditionally corresponds to CHAB and (b) frequency of bending vibration of CH_2 groups of hydroxyethylated gemini surfactants in solution.

Meanwhile, solubilization capacity of aggregates is one of the most important properties from the viewpoint of biomedicine applications. The ability of micelles and microemulsions to uptake the hydrophobic guests is widely used in design of drug delivery systems. Solubilization capacity can be characterized by the value of solubilization power (*S*): $S = b/\varepsilon$, where *b* is the slope of linear fragment corresponding to sharp increase in absorbance (Figure 5) and ε is the extinction coefficient equal to 17400 L mol^{-1} cm^{-1}. Resulting *S* values (Table 1) are markedly higher as compared to the typical single head cationic surfactant with trimethylammonium headgroup and hexadecyl tail.[96] The latter provides evidence that gemini under study can be recommended for further testing as effective drug carriers.

3.7. FTIR Spectroscopic Characterization of Gemini Surfactants in Solution. The spectrum of solid film of gemini surfactants exemplified by 16-12-16(OH) (Figure S11) shows peaks at 2850 and 2918 cm^{-1} (symmetric and asymmetric stretching, methylene group of alkyl chain), 2870 and 2950 cm^{-1} (symmetric and asymmetric stretching, methyl group of alkyl chain), 1467 cm^{-1} (scissoring, CH_2 bending), 1378 cm^{-1} (bending, CH_3 groups which are attached directly to the nitrogen), and 1160 and 978 cm^{-1} (stretching, CN^+). Doublet at 1050 and 1090 cm^{-1} is assigned to symmetric and antisymmetric C−O(H) stretching vibrations, respectively, due to the presence of hydroxyethyl groups. Intensity of the 1484 cm^{-1} shoulder (Figure 6) is proportional to the number of CH_3-groups in choline fragments of the samples.[97] This band in the spectrum of CHAB is relatively more intense due to less content of methylene groups.

The FTIR spectra analysis of gemini surfactants with systematically increasing spacer length helps to disclose some details of conformational properties of the samples in solution.

The employed surfactant concentrations (5 mM) significantly beyond the CMC values for all the surfactants studied, thus ensuring that all of them are in a micellized state. Different ordering of surfactant aliphatic chains in micelles manifests itself in the spectra of CH_2 bending vibrations (Figure 6) which is very sensitive to the interchain interactions. Frequency position of main absorbance maxima displays the aliphatic tails ordering,[97,98] as well as their accessibility to water.[99] As could be deduced from the results shown in Figure 6, the samples with increasing spacer length exhibit a shift to lower frequencies. The decrease of methylene groups bending frequency may result from their less ordering, higher hydration, or the both. CHAB exhibits the most ordered and least hydrated conformation among others. It could be assumed that upon the increasing of spacer length, the aliphatic groups became more loosely packed and more hydrated in micelles. This is in good agreement with results obtained by other techniques. In particular, a looser packing mode of gemini with longer spacers characterized by the moister interior correlates well with more polar microenvironvent of fluorescent dye Prodan (Figure 4) and lower solubilization capacity toward hydrophobic dye Orange OT (Figure 5). This is also consistent with the more expanded location of 16-12-16(OH) at the water/solution interface compared to gemini with a shorter spacer (Table 1).

3.8. Interaction of Surfactants with Lipid Bilayer. One of the most important characteristics of surfactants is their ability for integrating with lipid bilayer, which roughly correlates with their overcoming the biological barriers, such as cell membranes. To testify this property, the temperature of main phase transition or melting point (T_m) of liposomes based on DPPC was monitored by a turbidimetry technique, with the surfactant/lipid molar ratio varied. This method is based on the known fact that T_m value of lipids may be markedly influenced by addition of foreign compounds, including surfactants. For the DPPC bilayer, the temperature of liquid crystal to gel phase is documented to equal 41 ± 0.1 °C, which corresponds to the inflection point on the turbidimetry plot (Figure S12). The change of this parameter upon the surfactant added indicates the ordering (when T_m increase) or disordering (when T_m decrease) of the bilayer, thereby confirming the insertion of surfactant molecules into the lipid membrane. Recently, strong dependence of the interaction of gemini 16-s-16(OH) with DPPC bilayer on the spacer length has been documented.[29] In particular, only for gemini with the longest spacer 16-12-16(OH), the ability of integrating with DPPC bilayer was demonstrated, which was postulated as one of the key factors responsible for its high transfection efficacy.

To shed light on the structural factor determining interaction of gemini with DPPC bilayer, additional experiments were carried out, with the series of gemini extended and surfactant/lipid ratio enlarged (Figure 7). It was shown that structural characteristics, i.e., spacer length and hydrophobicity of gemini play an important role, determining their integrating with lipid bilayer, and thereby their ability of crossing lipid membranes. Unlike single head analog CHAB and gemini with a shorter spacer (*s* = 4, 6),[29,100] gemini with longer spacer (*s* = 10, 12) result in a decrease in lipid melt point, i.e., disordering

DOI: 10.1021/acs.jpcc.9b10079
J. Phys. Chem. C 2020, 124, 2178−2192

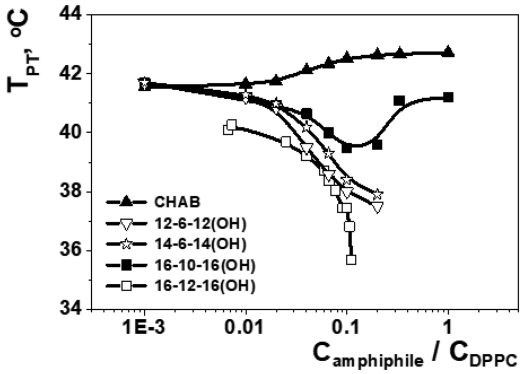

Figure 7. DPPC phase transition temperature as a function of surfactant-to-lipid molar ratio.

the membrane and promoting the transition from gel to liquid crystalline phase. The same is observed for the transition from longer to shorter alkyl tails, which is exemplified by a series of gemini with a hexamethylene spacer and different alkyl tails (Figure 7). While gemini 16-6-16(OH) has practically zero effect on T_m,[29] its less hydrophobic homologues strongly affect this parameter. Meanwhile, monitoring of changes in T_m for gemini with longer spacer exemplified by 16-10-16(OH) demonstrates that the T_m value after the initial decrease becomes an increase, testifying that the stabilization of a gel phase occurs. This is probably due to the fact that upon the addition of a small amount of surfactants, their tails loosen the alkyl tails of lipid molecules, while upon the increase in total concentration of amphiphilic molecules (lipid and surfactant) their closer packing occurs, thereby resulting in an ordering effect.

3.9. Complexation with Oligonucleotide. In our previous studies,[29,30] a high transfection efficacy of hydroxyethylated surfactants was documented, with 16-12-16(OH) demonstrating superior activity over other analogs. To model the nucleic acid-cationic surfactant interactions we examine the complexation of a DNA decamer with a hydroxyethylated gemini. The size of ONu-surfactant complexes (lipoplexes) was monitored at different component ratios (Figure 8). As can be seen, even very small surfactant additives result in crucial structural rearrangements in the system in all cases studied, which are evident from a sharp increase in sizes of lipoplexes. While single components demonstrate hydrodynamic diameter D_H < 10 nm, mixed systems are characterized by D_H of 70 to 150 nm, with sizes increasing at a component ratio approaching to 1. Around the ONu-surfactant equimolar ratio, bimodal size distribution appears followed by precipitation. Noteworthy that gemini induce the structural rearrangement at lower molar ratio of components as compared to single-head surfactant CHAB (Figure 8). In accordance with literature data,[101−103] population at 70−150 nm is probably due to the micelle-to-vesicle transition induced by oligonucleotide. In general, the structure of surfactants influences little the size behavior of lipoplexes under study. What is noteworthy is that at high surfactant concentrations, larger aggregates of microscale population can be observed (Figure 8), while no extremum-type dependence occurred, which was documented in some work[104] due to a reentrant condensation effect. This can be due to the fact that the

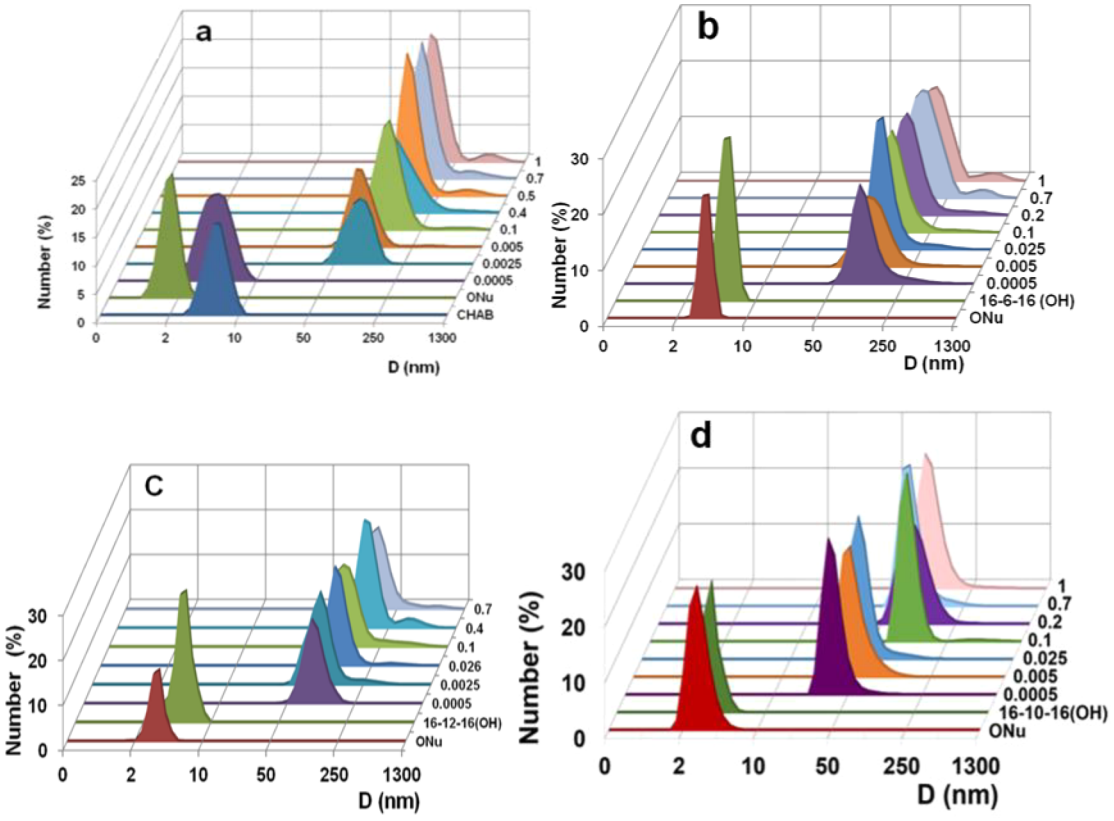

Figure 8. Number-averaged size distribution in single and mixed cationic surfactant-ONu systems at different molar ratio of components (see right axis). (a) CHAB, (b) 16-6-16(OH), (c) 16-12-16(OH), and (d) 16-10-16 (OH); 25 °C.

DOI: 10.1021/acs.jpcc.9b10079
J. Phys. Chem. C 2020, 124, 2178−2192

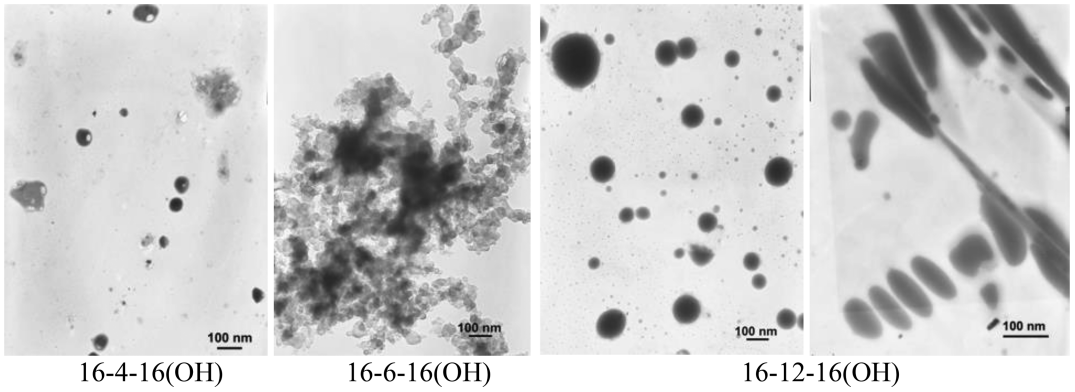

Figure 9. TEM photo of particles formed in 16-*s*-16-ONu samples.

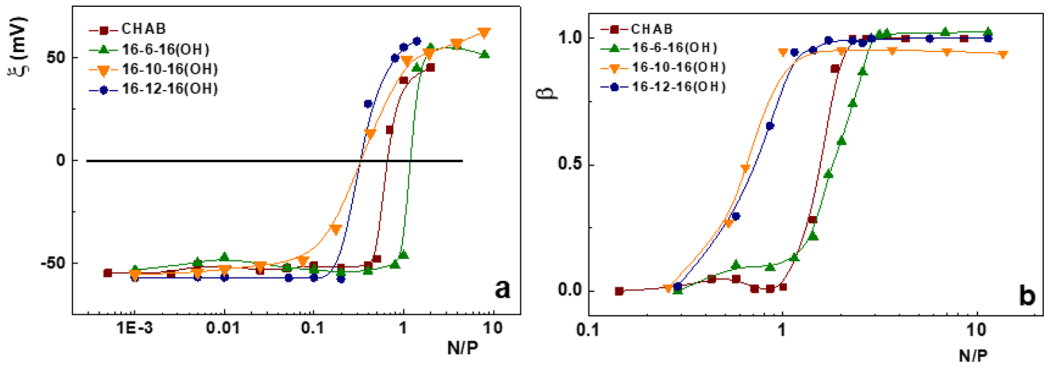

Figure 10. (a) Zeta potential data for cationic surfactant-ONu systems at different N/P molar ratio; 25 °C and (b) the binding degree of surfactants with oligonucleotide versus N/P ratio; 25 °C.

uniform size distribution in Figure 8 reflects the uniform charge distribution typical for a short oligonucleotide chain.

Additional information on size of lipoplexes was obtained from TEM images (Figure 9). For gemini with s = 4, 6, roughly spherical particles exist, with agglomeration observed in the case of s = 6. Unlike with those, two types of particles are formed in the case of 16-12-16(OH), i.e., spheres of different sizes and elongate rodlike structures. As a whole, sizes determined by DLS and TEM methods are in good agreement and supplement each other.

Zeta potential measurements strongly support the electrostatic character of ONu-surfactant complexation. An increase in the surfactant versus ONu ratio results in charge neutralization, in particular, zeta potential changes from ca. −54 mV to ca. + 50 mV (Figure 10). The N/P ratios (r_o) corresponding to zero-potential points equal 0.3 [16-10-16(OH) and 16-12-16(OH)); 0.6 (CHAB) and 1.2 (16-6-16(OH)]. This means that the highest electrostatic contribution is observed in the pairs 16-10-16(OH)-ONu and 16-12-16(OH)-ONu, while 16-6-16(OH) is less effective as compared to all three gemini analogs and monocationic counterparts. The weaker charge neutralization effect of gemini 16-6-16(OH) compared to other compounds may be due to (1) the predomination of the hydrophobic effect and hydrogen bonding over electrostatic contribution; or (2) the lower mutual affinity of 16-6-16(OH) and the oligonucleotide. Meanwhile, for unsubstituted analog 16-6-16, the r_o value is ∼0.631, i.e., the latter interacts with oligonucleotide more effectively.

To test the effectiveness of the ONu-surfactant complexation, the ethidium bromide exclusion is studied. This technique is based on the measurements of the fluorescence intensity of the EB that markedly increases due to its intercalation into nucleotide fragments of DNA. Competitive binding of oligonucleotide with surfactants results in the exclusion of EB and quenching the fluorescence. Fluorescence emission spectra of the systems studied are exemplified in Figure S13. These data were used to calculate the fraction of the bound oligonucleotide with the following equation: $\beta = (I_b - I_{obs})/(I_b - I_f)$, where I_f and I_b are the intensity of fluorescence of free EB and that bound with ONu, while I_{obs} is the observed intensity in titration measurements. Calculations show that the effective ONu-surfactant binding occurs beyond the equimolar component ratio (Figure 10).

It could be seen, that the effectiveness of the lipoplex formation changes in following the order 16-10-16(OH) > 16-12-16(OH) > CHAB > 16-6-16(OH). This indicates that the latter gemini demonstrates the lowest complexation capacity toward oligonucleotide. It should be remembered that the analogous order was obtained in the case of transfection efficacy mediated by gemini under study.[29,30] Taking into account the comparable or even superior effectiveness of the single-head cationic surfactant CHAB compared to hydroxyethylated short-bridged gemini, one can assume that the geometry factor probably plays a key role in the complexation. Elongation of the oligomethylene spacer of gemini could be used as a tool for an increase of its complexation capability with ONu and achieve quantitative binding of components at lower surfactant additives; however, this effect is nonmonotonous and bridge length should be selected very accurately.

DOI: 10.1021/acs.jpcc.9b10079
J. Phys. Chem. C 2020, 124, 2178−2192

Indeed, unlike shorter tetra- and hexametylene spacer fragments, monocationic analog and 16-12-16(OH) may provide conditions for the suitable orientation of molecules upon their interactions. The lipoplex formation is visualized in Figure 11, which shows the confocal microscope images

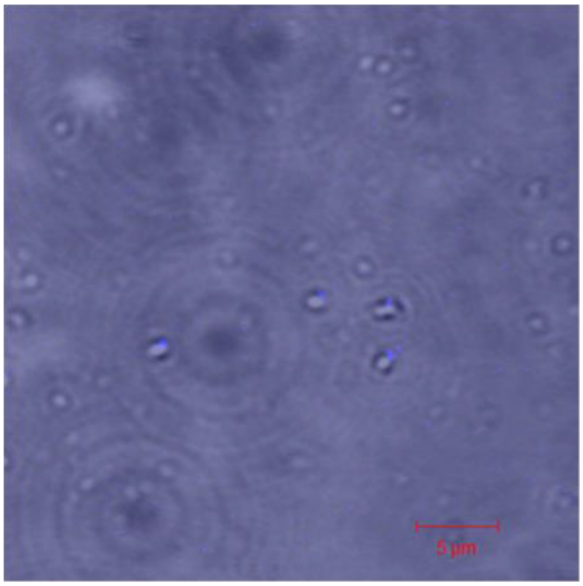

Figure 11. Confocal microscope images of lipoplexes formed in ONu-16-12-16(OH) system prior to the charge neutralization point; $C_{16\text{-}12\text{-}16(OH)}$ = 0.17 mM; C_{ONu} = 1 mM. The merged images represent a combination of two channels (Hoechst33342-blue and transmitted light channel).

exemplified by ONu-16-12-16(OH) system prior to the charge neutralization point. Beyond this point the precipitation occurs that is evident in Figure S14.

3.10. ATP-Gemini Interaction. To further shed light on interactions between components and on the molecular fragments responsible for complexation, ATP-gemini binary systems were studied by the NMR self-diffusion technique. Addition of ATP (0.5 mM) is shown to markedly affect the self-assembly behavior of gemini, with this effect increasing as spacer length increases. For example, for a 1 mM sample of 16-12-16(OH) in the absence and presence of ATP, the D_S and R_H values change from 0.72 × 10^{-10} to 0.45 × 10^{-10} m^2/s and from 3.9 to 6.1 nm, respectively. Analysis of self-diffusive data of the guest and host molecules proves that they are completely bound in these conditions, while upon the analysis of chemical shifts of guest protons one can conclude that the adenosine fragment was involved in the interaction, for which larger complexation induced shifts (CIS) values are observed compared to the sugar moiety. This is also strongly supported by the NOESY data (Figure 12a): there are cross-peaks between the adenosine fragment and hydrocarbon tail protons due to their close proximity. These data allow us to suppose the structure of the complex, in which ATP is bound to the surfactant aggregate without deep immersion inside the particle (Figure 12b). In this case, negatively charged phosphate residues are exposed to water and contribute to electrostatic interaction of components.

4. CONCLUSIONS

Aggregation behavior of hydroxyethylated gemini surfactants with different spacer fragments 16-*s*-16(OH) (*s* = 4, 6, 10, and 12) and their complexes with oligonucleotide was studied by different techniques. Due to a very low concentration threshold of aggregation, two types of aggregates are probably formed in hydroxyethylated gemini systems. Importantly, a high solubilization capacity of gemini toward the hydrophobic probe is testified, which makes it possible to recommend them for further testing as effective drug carriers. Compound 16-12-16(OH) demonstrates superior binding capacity toward oligonucleotide as compared to single head surfactant and gemini counterparts with shorter spacers. This may be due to the key role of the geometry factor in the complexation, i.e., the complementary interactions between components. The effectiveness of oligonucleotide-surfactant complexation

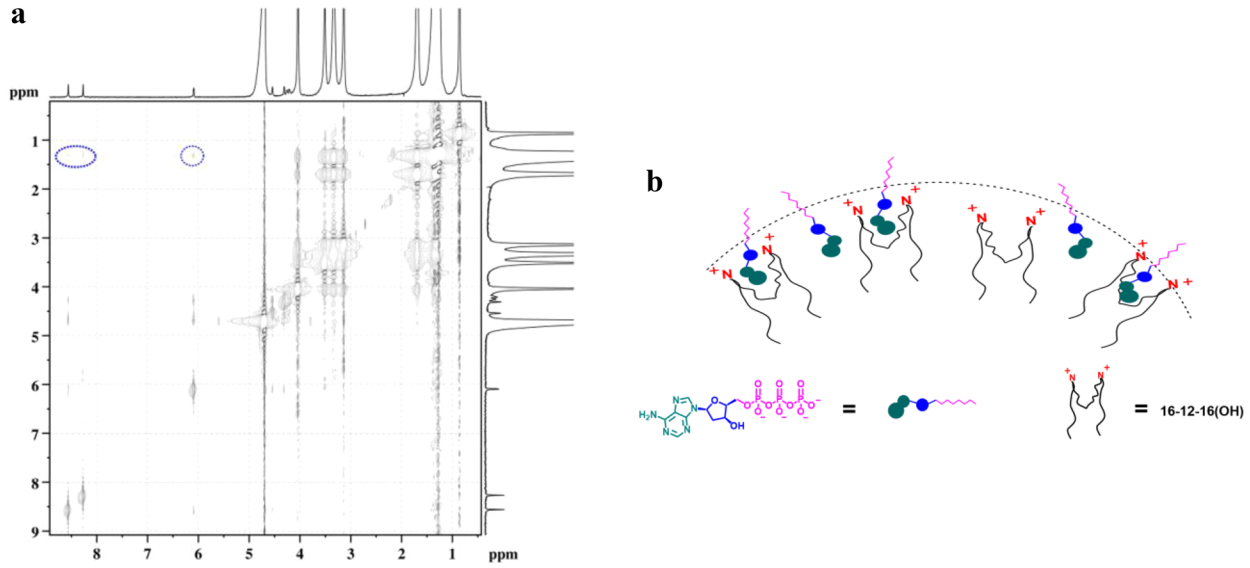

Figure 12. 2D NOESY NMR spectrum of mixture 16-12-16(OH) (5 mM) and ATP (1 mM) in D_2O, 303 K, mixing time of 200 ms. (a) NOE observed between adenosine protons of ATP and protons of aliphatic groups of surfactant are indicated by a circle. (b) Schematic representation of interaction between ATP and 16-12-16(OH) revealed by NMR experiments.

DOI: 10.1021/acs.jpcc.9b10079
J. Phys. Chem. C 2020, 124, 2178−2192

changes in the same order as transfection efficacy mediated by gemini reported earlier. These findings testify that hydroxyethylated gemini may be recommended as potential drug and gene carriers based on further detailed study.

■ ASSOCIATED CONTENT

Supporting Information

The Supporting Information is available free of charge at https://pubs.acs.org/doi/10.1021/acs.jpcc.9b10079.

Details of surface tension measurements, quantitative treatment of surface tension isotherms, fluorescence spectroscopy with the use of Pyrene, NMR experiment, fluorescence micropolarity study with the use of fluorescent dye Prodan, spectrophotometric assay of Orange OT solubilization, FTIR spectroscopic characterization of gemini surfactants in solution, turbidimetric measurements of surfactant/DPPC mixtures, description of sample preparation and the EB exclusion technique (PDF)

■ AUTHOR INFORMATION

Corresponding Author

*E-mail: luciaz@mail.ru. Fax: (+7843) 2732253. Tel: +7 (843) 273 22 93.

ORCID

Elmira A. Vasilieva: 0000-0002-1825-7803
Farida G. Valeeva: 0000-0002-7261-949X
Valery M. Zakharov: 0000-0002-3982-2277
Alexander R. Mukhitov: 0000-0001-6443-0788
Dzhigangir A. Faizullin: 0000-0002-2872-732X
Victor V. Syakaev: 0000-0002-3516-1969
Shamil K. Latypov: 0000-0003-4757-6157
Yuriy F. Zuev: 0000-0002-6715-2530
Lucia Ya. Zakharova: 0000-0002-2981-445X

Author Contributions

D.R.G., E.A.V., M.A.V., D.A.K., F.G.V., and A.B.M. performed the preparation of all samples for investigations, as well as the study on aggregation, membranotropic, and solubilization properties of amphiphiles. S.S.L. and V.M.Z. carried out the synthesis of amphiphilic compounds. A.R.M. and Vadim V.S. conducted studies using the microscopy techniques. D.A.F. and Y.F.Z. performed the FTIR measurements. Victor V.S. and S.K.L. carried out the NMR investigation. L.Y.Z. provided the fundamental plans and supervised the whole research project.

Notes

The authors declare no competing financial interest.

■ ACKNOWLEDGMENTS

L.Y.Z., D.R.G., D.A.K., F.G.V., A.B.M. and S.S.L. thank the Russian Science Foundation (project no. 19-73-30012) for financial support (self-assembly in single and binary systems, interaction with lipid bilayer). A.R.M., D.A.F., Vadim V.S., and Y.F.Z. thank the financial support from the government assignment for the FRC Kazan Scientific Center of RAS (FTIR study, visualization of lipoplexes). The authors gratefully acknowledge the Assigned Spectral-Analytical Center of FRC Kazan Scientific Center of RAS. Electron microscopy was carried out in the Interdisciplinary Center of Analytical Microscopy (Kazan Federal University).

■ REFERENCES

(1) Gao, Ch.; Bhattarai, P.; Chen, M.; Zhang, N.; Hameed, S.; Yue, X.; Dai, Zh. Amphiphilic drug conjugates as nanomedicines for combined cancer therapy. *Bioconjugate Chem.* **2018**, *29* (12), 3967−3981.

(2) Sharma, V. K.; Hayes, D. G.; Gupta, S.; Urban, V. S.; O'Neill, H. M.; Pingali, S. V.; Ohl, M.; Mamontov, E. Incorporation of melittin enhances interfacial fluidity of bicontinuous microemulsions. *J. Phys. Chem. C* **2019**, *123*, 11197−11206.

(3) Dias, R. S. *DNA interactions with polymers and surfactants*; John Wiley & Sons, Inc., 2008.

(4) Bhattacharya, S.; Bajaj, A. Advances in gene delivery through molecular design of cationic lipids. *Chem. Commun.* **2009**, *31*, 4632−4656.

(5) Kumar, M.; Jinturkar, K.; Yadav, M. R.; Misra, A. Gemini amphiphiles: a novel class of nonviral gene delivery vectors. *Crit. Rev. Ther. Drug Carrier Syst.* **2010**, *27* (3), 237−278.

(6) Wettig, S. D.; Verrall, R. E.; Foldvari, M. Gemini surfactants: a new family of building blocks for non-viral gene delivery systems. *Curr. Gene Ther.* **2008**, *8* (1), 9−23.

(7) Costa, D. M.; Miguel, G.; Lindman, B. Swelling properties of cross-linked DNA gels. *Adv. Colloid Interface Sci.* **2010**, *158*, 21−31.

(8) González-Pérez, A. Reversible DNA compaction. *Curr. Top. Med. Chem.* **2014**, *14* (6), 766−773.

(9) Bilalov, A.; Olsson, U.; Lindman, B. Complexation between DNA and surfactants and lipids: Phase behavior and molecular organization. *Soft Matter* **2012**, *8* (43), 11022−11033.

(10) Samarkina, D. A.; Gabdrakhmanov, D. R.; Lukashenko, S. S.; Khamatgalimov, A. R.; Kovalenko, V. I.; Zakharova, L. Ya. Cationic amphiphiles bearing imidazole fragment: From aggregation properties to potential in biotechnologies. *Colloids Surf., A* **2017**, *529*, 990−997.

(11) Zakharova, L.; Kashapov, R.; Vagapova, G.; Gabdrakhmanov, D.; Vasilieva, E. Comparative study of aqueous solutions of cationic surfactants: structure/activity relation in their aggregation and solubilization behavior and complexation with oligonucleotide. *Chem. Lett.* **2012**, *41* (10), 1226−1228.

(12) Mirgorodskaya, A. B.; Yackevich, E. I.; Gabdrakhmanov, D. R.; Lukashenko, S. S.; Zuev, Yu. F.; Zakharova, L. Ya. Self-organization and lipoplex formation of cationic surfactants with morpholinium head group. *J. Mol. Liq.* **2016**, *220*, 992−998.

(13) Zakharova, L. Ya.; Kaupova, G. I.; Gabdrakhmanov, D. R.; Gaynanova, G. A.; Ermakova, E. A.; Mukhitov, A. R.; Galkina, I. V.; Cheresiz, S. V.; Pokrovsky, A. G.; Skvortsova, P. V.; et al. Alkyl triphenylphosphonium surfactants as nucleic acid carriers: complexation efficacy toward DNA decamer, interaction with lipid bilayer and cytotoxicity study. *Phys. Chem. Chem. Phys.* **2019**, *21*, 16706−16717.

(14) Kuznetsova, D. A.; Gabdrakhmanov, D. R.; Lukashenko, S. S.; Voloshina, A. D.; Sapunova, A. S.; Kashapov, R. R.; Zakharova, L. Ya. Self-assembled systems based on novel hydroxyethylated imidazolium-containing amphiphiles: Interaction with DNA decamer, protein and lipid. *Chem. Phys. Lipids* **2019**, *223*, 104791.

(15) Kuznetsova, D. A.; Gabdrakhmanov, D. R.; Lukashenko, S. S.; Voloshina, A. D.; Sapunova, A. S.; Kulik, N. V.; Nizameev, I. R.; Kadirov, M. K.; Kashapov, R. R.; Zakharova, L. Ya. Supramolecular systems based on cationic imidazole-containing amphiphiles bearing hydroxyethyl fragment: Aggregation properties and functional activity. *J. Mol. Liq.* **2019**, *289*, 111058.

(16) Zakharova, L. Ya.; Vasilieva, E. A.; Gabdrakhmanov, D. R.; Konovalov, A. I.; Zuev, Yu. F. Complexation of mono- and dicationic surfactants with decanucleotide. Influence of the head group nature. *Russ. Chem. Bull.* **2014**, *63* (7), 1615−1618.

(17) Zhou, T.; Xu, G.; Ao, M.; Yang, Y.; Wang, Ch. DNA compaction to multi-molecular DNA condensation induced by cationic imidazolium gemini surfactants. *Colloids Surf., A* **2012**, *414*, 33−40.

(18) Bhadani, A.; Singh, S. Synthesis and properties of thioether spacer containing gemini imidazolium surfactants. *Langmuir* **2011**, *27*, 14033−14044.

DOI: 10.1021/acs.jpcc.9b10079
J. Phys. Chem. C 2020, 124, 2178−2192

(19) Kamboj, R.; Singh, S.; Bhadani, A.; Kataria, H.; Kaur, G. Gemini imidazolium surfactants: synthesis and their biophysiochemical study. *Langmuir* **2012**, *28*, 11969−11978.
(20) Zhou, T.; Llizo, A.; Li, P.; Wang, C.; Guo, Y.; Ao, M.; Bai, L.; Wang, C.; Yang, Y.; Xu, G. High transfection efficiency of homogeneous DNA nanoparticles induced by imidazolium gemini surfactant as nonviral vector. *J. Phys. Chem. C* **2013**, *117*, 26573−26581.
(21) Sharma, V. D.; Aifuwa, E. O.; Heiney, P. A.; Ilies, M. A. Interfacial engineering of pyridinium gemini surfactants for the generation of synthetic transfection systems. *Biomaterials* **2013**, *34*, 6906−6921.
(22) Yaseen, Z.; Rehman, S. U.; Tabish, M.; Kabir-ud-Din. Interaction between DNA and cationic diester-bonded Gemini surfactants. *J. Mol. Liq.* **2014**, *197*, 322−327.
(23) Mirgorodskaya, A.; Yackevich, E.; Syakaev, V.; Latypov, Sh.; Zakharova, L.; Konovalov, A. Micellization and catalytic properties of cationic surfactants with head groups functionalized with a hydroxyalkyl fragment. *J. Chem. Eng. Data* **2012**, *57*, 3153−3163.
(24) Mirgorodskaya, A. B.; Yackevich, E. I.; Zakharova, L.Ya.; Konovalov, A. I. Oil-in-water microemulsions based on cationic surfactants with a hydroxyalkyl fragment in the head group. *Chem. Phys. Lett.* **2013**, *567*, 18−22.
(25) Sharma, V.; Borse, M.; Aswal, V. K.; Pokhriyal, N. K.; Joshi, J. V.; Goyal, P. S.; Devi, S. Synthesis, characterization, and SANS studies of novel alkanediyl-α,ω-bis(hydroxyethylmethylhexadecylammonium bromide) cationic gemini surfactants. *J. Colloid Interface Sci.* **2004**, *277*, 450−455.
(26) Kumar, B.; Tikariha, D.; Ghosh, K. K.; Barbero, N.; Quagliotto, P. Effect of polymers and temperature on critical micelle concentration of some gemini and monomeric surfactants. *J. Chem. Thermodyn.* **2013**, *62*, 178−185.
(27) Dasgupta, A.; Das, P. K.; Dias, R. S.; Miguel, M. G.; Lindman, B.; Jadhav, V. M.; Gnanamani, M.; Maiti, S. Effect of headgroup on DNA-cationic surfactant interactions. *J. Phys. Chem. B* **2007**, *111*, 8502−8508.
(28) Tiwari, A. K.; Sonu; Saha, S. K. Effect of hydroxyl group substituted spacer group of cationic gemini surfactants on solvation dynamics and rotational relaxation of Coumarin-480 in aqueous micelles. *J. Phys. Chem. B* **2014**, *118*, 3582−3592.
(29) Zakharova, L.; Gabdrakhmanov, D.; Ibragimova, A.; Vasilieva, E.; Nizameev, I.; Kadirov, M.; Pokrovsky, A.; Korobeynikov, V.; Cheresiz, S.; Ermakova, E.; et al. Structural, biocomplexation and gene delivery properties of hydroxyethylated gemini surfactants: Role of spacer length. *Colloids Surf., B* **2016**, *140*, 269−277.
(30) Grigoriev, I. V.; Korobeinikov, V. A.; Cheresiz, S. V.; Pokrovsky, A. G.; Zakharova, L. Y.; Voronin, M. A.; Lukashenko, S. S.; Konovalov, A. I.; Zuev, Y. F. Cationic gemini surfactants as new agents for plasmid DNA delivery into cells. *Dokl. Biochem. Biophys.* **2012**, *445* (1), 197−199.
(31) Dias, R. S.; Magno, L. M.; Valente, A. J.; Das, D.; Das, P. K.; Maiti, S.; Miguel, M. G.; Lindman, B. Interaction between DNA and cationic surfactants: effect of DNA conformation and surfactant headgroup. *J. Phys. Chem. B* **2008**, *112*, 14446−14452.
(32) Chauhan, V.; Singh, S.; Kamboj, R.; Mishra, R.; Kaur, G. Self-assembly, DNA binding and cytotoxicity trends of ether functionalized gemini pyridinium amphiphiles. *J. Colloid Interface Sci.* **2014**, *417*, 385−395.
(33) Pullmannová, P.; Funari, S. S.; Devínsky, F.; Uhríková, D. The DNA−DNA spacing in gemini surfactants−DOPE−DNA complexes. *Biochim. Biophys. Acta, Biomembr.* **2012**, *1818*, 2725−2731.
(34) Bajaj, A.; Kondiah, P.; Bhattacharya, S. Design, synthesis, and *in vitro* gene delivery efficacies of novel cholesterol-based gemini cationic lipids and their serum compatibility: a structure-activity investigation. *J. Med. Chem.* **2007**, *50*, 2432−2442.
(35) Bajaj, A.; Paul, B.; Kondaiah, P.; Bhattacharya, S. Structure-activity investigation on the gene transfection properties of cardiolipin mimicking gemini lipid analogues. *Bioconjugate Chem.* **2008**, *19*, 1283−1300.
(36) Biswas, J.; Mishra, S. K.; Kondaiah, P.; Bhattacharya, S. Syntheses, transfection efficacy and cell toxicity properties of novel cholesterol-based gemini lipids having hydroxyethyl head group. *Org. Biomol. Chem.* **2011**, *9*, 4600−4613.
(37) Munoz-Ubeda, M.; Misra, S. K.; Barran-Berdon, A. L.; Datta, S.; Aicart-Ramos, C.; Castro-Hartmann, P.; Kondaiah, P.; Junquera, E.; Bhattacharya, S.; Aicart, E. How does the spacer length of cationic gemini lipids influence the lipoplex formation with plasmid DNA? Physicochemical and biochemical characterizations and their relevance in gene therapy. *Biomacromolecules* **2012**, *13*, 3926−3937.
(38) Biswas, J.; Bajaj, A.; Bhattacharya, S. Membranes of cationic gemini lipids based on cholesterol with hydroxyl headgroups and their interactions with DNA and phospholipid. *J. Phys. Chem. B* **2011**, *115*, 478−486.
(39) Bajaj, A.; Kondaiah, P.; Bhattacharya, S. Gene transfection efficacies of novel cationic gemini lipids possessing aromatic backbone and oxyethylene spacers. *Biomacromolecules* **2008**, *9*, 991−999.
(40) Zana, R. Dimeric (gemini) surfactants: effect of the spacer group on the association behavior in aqueous solution. *J. Colloid Interface Sci.* **2002**, *248*, 203−220.
(41) Tehrani-Bagha, A. R.; Holmberg, K.; Nyden, M.; Nordstierna, L. Micelle growth of cationic gemini surfactants studied by NMR and by time-resolved fluorescence quenching. *J. Colloid Interface Sci.* **2013**, *405*, 145−149.
(42) Martín, V. I.; Rodríguez, A.; Laschewsky, A.; Moyá, M. L. Self-aggregation of cationic dimeric surfactants in water−ionic liquid binary mixtures. *J. Colloid Interface Sci.* **2014**, *430*, 326−336.
(43) Laschewsky, A.; Lunkenheimer, K.; Rakotoaly, R. H.; Wattebled, L. Spacer effects in dimeric cationic surfactants. *Colloid Polym. Sci.* **2005**, *283*, 469−479.
(44) Tavano, L.; Infante, M. R.; Riya, M. A.; Pinazo, A.; Vinardell, M. P.; Mitjans, M.; Manresa, M. A.; Perez, L. Role of aggregate size in the hemolytic and antimicrobial activity of colloidal solutions based on single and gemini surfactants from arginine. *Soft Matter* **2013**, *9*, 306−319.
(45) Sakai, K.; Nomura, K.; Shrestha, R. G.; Endo, T.; Sakamoto, K.; Sakai, H.; Abe, M. Effects of spacer chain length of amino acid-based gemini surfactants on wormlike micelle formation. *J. Oleo Sci.* **2014**, *63* (3), 249−255.
(46) Zhiltsova, E. P.; Pashirova, T. N.; Ibatullina, M. R.; Lukashenko, S. S.; Gubaidullin, A. T.; Islamov, D. R.; Kataeva, O. N.; Kutyreva, M. P.; Zakharova, L. Ya. New surfactant-copper(II) complex based on 1,4-diazabicyclo[2.2.2]octane amphiphile. Crystal structure determination, self-assembly and functional activity. *Phys. Chem. Chem. Phys.* **2018**, *20* (18), 12688−12699.
(47) Lopez-Lopez, M.; Lopez-Cornejo, P.; Martin, V. I.; Ostos, F. J.; Checa-Rodriguez, C.; Prados-Carvajal, R.; Lebron, J. A.; Huertas, P.; Moya, M. L. Importance of hydrophobic interactions in the single-chained cationic surfactant-DNA complexation. *J. Colloid Interface Sci.* **2018**, *521*, 197−205.
(48) Shortall, S. M.; Wettig, S. D. Cationic gemini surfactant−plasmid deoxyribonucleic acid condensates as a single amphiphilic entity. *J. Phys. Chem. B* **2018**, *122* (1), 194−199.
(49) Kasyanenko, N.; Unksov, I.; Bakulev, V.; Santer, S. DNA Interaction with head-to-tail associates of cationic surfactants prevents formation of compact particles. *Molecules* **2018**, *23* (7), 1576.
(50) Guo, Q.; Zhang, Zh.; Song, Y.; Liu, Sh.; Gao, W.; Qiao, H.; Guo, L.; Wang, J. Investigation on interaction of DNA and several cationic surfactants with different head groups by spectroscopy, gel electrophoresis and viscosity technologies. *Chemosphere* **2017**, *168*, 599−605.
(51) Damen, M.; Groenen, A. J. J.; Van Dongen, S.F. M.; Nolte, R. J. M.; Scholte, B. J.; Feiters, M. C. Transfection by cationic gemini lipids and surfactants. *MedChemComm* **2018**, *9* (9), 1404−1425.
(52) Puchkov, P. A.; Kartashova, I. A.; Shmendel, E. V.; Luneva, A. S.; Morozova, N. G.; Zenkova, M. A.; Maslov, M. A. Spacer structure and hydrophobicity influences transfection activity of novel polycationic gemini amphiphiles. *Bioorg. Med. Chem. Lett.* **2017**, *27*, 3284−3288.

DOI: 10.1021/acs.jpcc.9b10079
J. Phys. Chem. C 2020, 124, 2178−2192

(53) Sarrión, B.; Bernal, E.; Martín, V. I.; López-López, M.; López-Cornejo, P.; García-Calderón, M.; Moyá, M. L. Binding of 12-s-12 dimeric surfactants to calf thymus DNA: Evaluation of the spacer length influence. *Colloids Surf., B* **2016**, *144*, 311−318.
(54) Martínez-Negro, M.; Barrán-Berdón, A. L.; Aicart-Ramos, C.; Moyá, M. L.; de Ilarduya, C. T.; Aicart, E.; Junquera, E. Transfection of plasmid DNA by nanocarriers containing a gemini cationic lipid with an aromatic spacer or its monomeric counterpart. *Colloids Surf., B* **2018**, *161*, 519−527.
(55) Zakharova, L.; Voronin, M.; Semenov, V.; Gabdrakhmanov, D.; Syakaev, V.; Gogolev, Y.; Giniyatullin, R.; Lukashenko, S.; Reznik, V.; Latypov, S.; Konovalov, A.; Zuev, Y. Supramolecular systems based on novel mono- and dicationic pyrimidinic amphiphiles and oligonucleotides: a self-organization and complexation study. *ChemPhysChem* **2012**, *13*, 788−796.
(56) Gabdrakhmanov, D. R.; Voronin, M. A.; Zakharova, L. Ya.; Konovalov, A. I.; Khaybullin, R. N.; Strobykina, I. Yu.; Kataev, V. E.; Faizullin, D. A.; Gogoleva, N. E.; Konnova, T. A.; et al. Supramolecular design of biocompatible nanocontainers based on amphiphilic derivatives of a natural compound isosteviol. *Phys. Chem. Chem. Phys.* **2013**, *15*, 16725−16735.
(57) Voronin, M. A.; Gabdrakhmanov, D. R.; Khaibullin, R. N.; Strobykina, I. Yu.; Kataev, V. E.; Idiyatullin, B. Z.; Faizullin, D. A.; Zuev, Yu. F.; Zakharova, L. Ya.; et al. Novel biomimetic systems based on amphiphilic compounds with a diterpenoid fragment: Role of counterions in self-assembly. *J. Colloid Interface Sci.* **2013**, *405*, 125−133.
(58) Mirgorodskaya, A. B.; Yackevich, E. I.; Lukashenko, S. S.; Zakharova, L. Y.; Konovalov, A. I. Solubilization and catalytic behavior of micellar system based on gemini surfactant with hydroxyalkylated head group. *J. Mol. Liq.* **2012**, *169*, 106−109.
(59) Mirgorodskaya, A. B.; Bogdanova, L. R.; Kudryavtseva, L. A.; Lukashenko, S. S.; Konovalov, A. I. Role of surface potential in the catalytic action of micelles of cationic surfactants with a hydroxyalkyl fragment in the head group. *Russ. J. Gen. Chem.* **2008**, *78*, 163−170.
(60) Borse, M.; Sharma, V.; Aswal, V. K.; Goyal, P. S.; Devi, S. Effect of head group polarity and spacer chain length on the aggregation properties of gemini surfactants in an aquatic environment. *J. Colloid Interface Sci.* **2005**, *284*, 282−288.
(61) Wu, D.; Chen, A.; Johnson, C. S. An improved diffusion-ordered spectroscopy experiment incorporating bipolar-gradient pulses. *J. Magn. Reson., Ser. A* **1995**, *115*, 260−264.
(62) Cohen, Y.; Avram, L.; Frish, L. Diffusion NMR spectroscopy in supramolecular and combinatorial chemistry: an old parameter − new insights. *Angew. Chem., Int. Ed.* **2005**, *44*, 520−554.
(63) Pregosin, P. S.; Kumar, P. G.; Fernandez, I. Pulsed gradient spin−echo (PGSE) diffusion and ^{1}H, ^{19}F heteronuclear overhauser spectroscopy (HOESY) NMR methods in inorganic and organometallic chemistry: something old and something new. *Chem. Rev.* **2005**, *105*, 2977−2998.
(64) Brand, T.; Cabrita, E. J.; Berger, S. Intermolecular interaction as investigated by NOE and diffusion studies. *Prog. Nucl. Magn. Reson. Spectrosc.* **2005**, *46*, 159−196.
(65) Schott, H. Solubilization of a water-insoluble dye as a method for determining micellar molecular weights. *J. Phys. Chem.* **1966**, *70*, 2966−2973.
(66) Tachiya, M. Application of a generating function to reaction kinetics in micelles Kinetics of quenching of luminescent probes in micelles. *Chem. Phys. Lett.* **1975**, *33*, 289−292.
(67) Turro, N. J.; Yekta, A. Luminescent probes for detergent solutions. A simple procedure for determination of the mean aggregation number of micelles. *J. Am. Chem. Soc.* **1978**, *100*, 5951−5952.
(68) Kalyanasundaram, K.; Thomas, J. K. Environmental effects on vibronic band intensities in pyrene monomer fluorescence and their application in studies of micellar systems. *J. Am. Chem. Soc.* **1977**, *99*, 2039−2044.
(69) Menger, F. M.; Littau, C. A. Gemini surfactants: A new class of self-assembling molecules. *J. Am. Chem. Soc.* **1993**, *115*, 10083−10090.
(70) Menger, F. M.; Keiper, J. S. Gemini surfactants. *Angew. Chem., Int. Ed.* **2000**, *39*, 1906−1920.
(71) Hait, S. K.; Moulik, S. P. Gemini surfactants: A distinct class of self-assembling molecules. *Curr. Sci.* **2002**, *82*, 1101−1111.
(72) Aslam, J.; Siddiqui, U. S.; Bhat, I. A.; Kabir-ud-Din. Molecular interactions of cationic gemini surfactants (m-s-m) with an environmental friendly nonionic sugar-based surfactant (β-C12G): Interfacial, micellar and aggregation behavior. *J. Ind. Eng. Chem.* **2014**, *20*, 3841−3850.
(73) Hajy Alimohammadi, M.; Javadian, S.; Gharibi, H.; Tehrani-Bagha, A. r.; Alavijeh, M. R.; Kakaei, K. Aggregation behavior and intermicellar interactions of cationic Gemini surfactants: Effects of alkyl chain, spacer lengths and temperature. *J. Chem. Thermodyn.* **2012**, *44*, 107−115.
(74) Siddiqui, U. S.; Aslam, J.; Ansari, W. H.; Kabir-ud-Din. Micellization and aggregation behavior of a series of cationic gemini surfactants (m-*s*-m type) on their interaction with a biodegradable sugar-based surfactant (octyl-β-D-glucopyranoside). *Colloids Surf., A* **2013**, *421*, 164−172.
(75) Łudzik, K.; Piekarski, H.; Kubalczyk, K.; Wasiak, M. Micellization properties of cationic gemini surfactants in aqueous solution. *Thermochim. Acta* **2013**, *558*, 29−35.
(76) Bai, G.; Wang, J.; Yan, H.; Li, Zh.; Thomas, K. R. Thermodynamics of molecular self-assembly of cationic gemini and related double chain surfactants in aqueous solution. *J. Phys. Chem. B* **2001**, *105*, 3105−3108.
(77) Bernheim-Groswasser, A.; Zana, R.; Talmon, Y. Sphere-to-cylinder transition in aqueous micellar solution of a dimeric (gemini) surfactant. *J. Phys. Chem. B* **2000**, *104*, 4005−4009.
(78) Geng, Y.; Romsted, L. S.; Menger, F. Specific ion pairing and interfacial hydration as controlling factors in gemini micelle morphology. Chemical trapping studies. *J. Am. Chem. Soc.* **2006**, *128*, 492−501.
(79) Kuwamoto, K.; Asakawa, T.; Ohta, A.; Miyagishi, Sh. Degree of micelle ionization and micellar growth for gemini surfactants detected by 6-methoxy-N-(3-sulfopropyl)quinolinium fluorescence quenching. *Langmuir* **2005**, *21*, 7691−7695.
(80) Jiang, Y.; Chen, H.; Cui, X.-H.; Mao, S.-Zh.; Liu, M.-L.; Luo, P.-Y.; Du, Y.-R. ^{1}H NMR study on pre-micellization of quaternary ammonium gemini surfactants. *Langmuir* **2008**, *24*, 3118−3121.
(81) Borse, M. S.; Devi, S. Importance of head group polarity in controlling aggregation properties of cationic gemini surfactants. *Adv. Colloid Interface Sci.* **2006**, *123*, 387−399.
(82) Aguiar, J.; Carpena, P.; Molina-Bolívar, J. A.; Carnero Ruiz, C. On the determination of the critical micelle concentration by the pyrene 1:3 ratio method. *J. Colloid Interface Sci.* **2003**, *258*, 116−122.
(83) De, S.; Aswal, V. K.; Goyal, P. S.; Bhattacharya, S. Role of spacer chain length in dimeric micellar organization. small angle neutron scattering and fluorescence studies. *J. Phys. Chem.* **1996**, *100*, 11664−11671.
(84) Stilbs, P.; Lindman, B. Determination of organic counterion binding to micelles through Fourier transform NMR self-diffusion measurements. *J. Phys. Chem.* **1981**, *85*, 2587−2589.
(85) Macchioni, A.; Ciancaleoni, G.; Zuccaccia, C.; Zuccaccia, D. Determining accurate molecular sizes in solution through NMR diffusion spectroscopy. *Chem. Soc. Rev.* **2008**, *37*, 479−489.
(86) Garcia de la Torre, J.; Huertas, M. L.; Carrasco, B. HYDRONMR: Prediction of NMR relaxation of globular proteins from atomic-level structures and hydrodynamic calculations. *J. Magn. Reson.* **2000**, *147*, 138−146.
(87) Bogdanova, L. N.; Mchedlov-Petrossyan, N. O.; Vodolazkaya, N. A.; Lebed, A. V. The influence of beta-cyclodextrin on acid-base and tautomeric equilibrium of fluorescein dyes in aqueous solution. *Carbohydr. Res.* **2010**, *345*, 1882−1890.
(88) Vodolazkaya, N. A.; Mchedlov-Petrossyan, N. O.; Salamanova, N. V.; Surov, Y. N.; Doroshenko, A. O. Molecular spectroscopy

DOI: 10.1021/acs.jpcc.9b10079
J. Phys. Chem. C 2020, 124, 2178−2192

studies of solvent properties of dispersed 'water pools': Fluorescein and 2,7-dichlorofluorescein in reversed AOT-based microemulsions. *J. Mol. Liq.* **2010**, *157*, 105−112.
(89) Mohanty, A.; Patra, T.; Dey, J. Salt-induced vesicle to micelle transition in aqueous solution of sodium N-(4-*n*-octyloxybenzoyl)-L-valinate. *J. Phys. Chem. B* **2007**, *111*, 7155−7159.
(90) Mohanty, A.; Dey, J. Effect of the headgroup structure on the aggregation behavior and stability of self-assemblies of sodium *n*-[4-(*n*-dodecyloxy)benzoyl]-l-aminoacidates in water. *Langmuir* **2007**, *23*, 1033−1040.
(91) Khatua, D.; Dey, J. Fluorescence, circular dichroism, light scattering, and microscopic characterization of vesicles of sodium salts of three *n*-acyl peptides. *J. Phys. Chem. B* **2007**, *111*, 124−130.
(92) Mchedlov-Petrossyan, N. O.; Vodolazkaya, N. A.; Gurina, Y. A.; Sun, W.-C.; Gee, K. R. Medium effects on the prototropic equilibria of fluorescein fluoro derivatives in true and organized solution. *J. Phys. Chem. B* **2010**, *114*, 4551−4564.
(93) Vequi-Suplicy, C. C.; Coutinho, K.; Teresa Lamy, M. Optical characterization of Prodan aggregates in water medium. *Phys. Chem. Chem. Phys.* **2013**, *15*, 11800−11807.
(94) Daneri, M.; Abelt, C. J. A higher-order preferential solvation model for the fluorescence of two PRODAN derivatives in toluene-alcohol mixtures. *J. Photochem. Photobiol., A* **2015**, *310*, 106−112.
(95) Artukhov, V. Ya.; Zharkova, O. M.; Morozova, Ju. P. Features of absorption and fluorescence spectra of prodan. *Spectrochim. Acta, Part A* **2007**, *68*, 36−42.
(96) Gainanova, G. A.; Vagapova, G. I.; Syakaev, V. V.; Ibragimova, A. R.; Valeeva, F. G.; Tudriy, E. V.; Galkina, I. V.; Kataeva, O. N.; Zakharova, L. Ya.; Latypov, Sh. K.; et al. Self-assembling systems based on amphiphilic alkyltriphenylphosphonium bromides: Elucidation of the role of head group. *J. Colloid Interface Sci.* **2012**, *367*, 327−336.
(97) Li, Z.; Jiang, W.-T.; Hong, H. An FTIR investigation of hexadecyltrimethylammonium intercalation into rectorite. *Spectrochim. Acta, Part A* **2008**, *71*, 1525−1534.
(98) Viana, R. B.; da Silva, A. B. F.; Pimentel, A. S. Infrared spectroscopy of anionic, cationic, and zwitterionic surfactants. *Adv. Phys. Chem.* **2012**, *2012*, 1−14.
(99) Reichardt, C. *Solvents and Solvent effects in organic chemistry*; VCH, 1988.
(100) Kuznetsova, D. A.; Gabdrakhmanov, D. R.; Lukashenko, S. S.; Zakharova, L. Ya. Adsorption and membranotropic properties of colloid systems based on cationic amphiphiles: the effect of the head group structure. *Russ. J. Phys. Chem. A* **2019**, *93* (8), 1584−1588.
(101) Guo, X.; Li, H.; Zhang, F.; Zheng, S.; Guo, R. Aggregation of single-chained cationic surfactant molecules into vesicles induced by oligonucleotide. *J. Colloid Interface Sci.* **2008**, *324*, 185−191.
(102) Liu, X.; Abbott, N. L. Characterization of the nanostructure of complexes formed by single- or double-stranded oligonucleotides with a cationic surfactant. *J. Phys. Chem. B* **2010**, *114*, 15554−15564.
(103) Santhiya, D.; Dias, R. S.; Shome, A.; Das, P. K.; Miguel, M. G.; Lindman, B.; Maiti, S. Role of linker groups between hydrophilic and hydrophobic moieties of cationic surfactants on oligonucleotide-surfactant interactions. *Langmuir* **2009**, *25*, 13770−13775.
(104) Sennato, S.; Bordi, F.; Cametti, C.; Diociaiuti, M.; Malaspina, P. Charge patch attraction and reentrant condensation in DNA-liposome complexes. *Biochim. Biophys. Acta, Biomembr.* **2005**, *1714*, 11−24.

DOI: 10.1021/acs.jpcc.9b10079
J. Phys. Chem. C 2020, 124, 2178−2192